International Journal of Electronics Signals and Systems

Volume 3 | Issue 2 Article 14

October 2013

A NOVEL MULTIPHASE BIDIRECTIONAL FLY-BACK CONVERTER TOPOLOGY IS APPLIED TO INDUCTION MOTOR DRIVE

M. RAMA MOHANA RAO
Department of Electrical and Electronics Engineering, Sri Vasavi Engineering College, Tadepalligudem, mohaneee6@gmail.com

C. H. RAMBABU
Department of Electrical and Electronics Engineering, Sri Vasavi Engineering College, Tadepalligudem, ram_feb7@rediffmail.com

A NOVEL MULTIPHASE BIDIRECTIONAL FLY-BACK CONVERTER TOPOLOGY IS APPLIED TO INDUCTION MOTOR DRIVE

M.RAMA MOHANA RAO[1] & CH.RAMBABU[2]

[1,2]Department of Electrical and Electronics Engineering, Sri Vasavi Engineering College, Tadepalligudem
E-mail: mohaneee6@gmail.com, ram_feb7@rediff.com

Abstract- Hybrid Electric Vehicle (HEV) is an emerging technology in the modern world because of the fact that it mitigates environmental pollutions and at the same time increases fuel efficiency of the vehicles. Bi-directional Fly – back Converter controls electric drive of HEV of high power and enhances its performance which is the reflection of the fact that it can generate Constant voltages. For hybrid electric vehicles, the batteries and the drive dc link may be at different voltages. The batteries are at low voltage to obtain higher volumetric efficiencies, and the dc link is at higher voltage to have higher efficiency on the motor side. Therefore, a power interface between the batteries and the drive's dc link is essential. This power interface should handle power flow from battery to motor, motor to battery, external gen-set to battery, and grid to battery. This paper proposes a multi-power-port topology which is capable of handling multiple power sources and still maintains simplicity and features like obtaining high gain, wide load variations, lower output-current ripple, and capability of parallel-battery energy due to the modular structure. The scheme incorporates a transformer winding technique which drastically reduces the leakage inductance of the coupled inductor. The development and testing of a bidirectional fly-back dc–dc converter for hybrid electric vehicle is described in this paper. Simple hysteresis voltage control is used for dc-link voltage regulation. The simulation results are presented, and modeling the circuit by using MATLAB/SIMULINK Platform.

Keywords: *Bidirectional fly-back converter, hybrid electric Vehicle, leakage inductance.*

I. INTRODUCTION

The ever-increasing need for oil combined with a worldwide increasing traffic density, regulatory requirements for reduced emissions, and the ongoing discussion about climate change present strong incentives for the automotive industry to further improve the car drive trains, to reduce fuel consumption, and to lower emissions of exhaust gases that are harmful to the environment, such as carbon dioxide. The required efficiency improvement can be achieved with a hybrid drive train which combines an electric motor and a combustion engine in a way that facilitates the most desirable operation of each [1]. One or more additional energy sources, such as high voltage (HV) batteries for continuous electric energy demand and ultra capacitors for high peak power [2], provide the electric power. Thus, in a hybrid electric vehicle, highly efficient and compact power electronic converters are required to provide the propulsion power and to facilitate the energy transfer between different dc voltage levels [3].

Now, the need for a bidirectional power converter should be properly examined. A battery can be used as a dc bus if the motor is rated for that voltage level. Thus, bidirectional power flow is not a problem because of the bidirectional power-handling capacity of a standard two-level three-phase inverter and also sinking and sourcing capacity of the battery. However, the traction motor should be rated for higher voltage to achieve higher efficiency for a given power rating. Therefore, the dc bus voltage should be maintained high enough to match the motor voltage rating. This problem can be solved by connecting a number of batteries in series. However, if too many batteries are connected in series, then the volumetric efficiency of the battery comes down. Therefore, there is a need for a bidirectional converter which interfaces the low-voltage battery with a high-voltage dc bus and maintains a bidirectional power flow.[2] shows the use of a bidirectional converter for a permanent-magnet ac motor- driven electric vehicle. [3] shows the use of a cascaded bidirectional buck–boost converter for the use in dc-motor-driven electric vehicle. Both schemes emphasize the importance of bidirectional dc–dc converter for electric vehicle application. The dc–dc converters can be divided into hard switching converters and soft-switching converters. Because of the low efficiency of hard-switching converters, recently, soft-switching techniques are getting popular. [4] proposes ZVS techniques for different non-isolated dc–dc converters. There is a limit on the voltage gain that can be achieved using a buck–boost or a boost converter. It is not desirable to operate the boost or the buck–boost converter at very high duty ratio because of very high capacitor current ripple. Thus, the solution is to go for isolated topologies for getting the high voltage gain in between the battery and the dc bus. In such topologies, any voltage gain can be achieved by setting the turns ratio of the transformers or the coupled inductors. Moreover, such topologies also provide the advantage of galvanic isolation between the battery bank and the dc bus. The recently proposed topologies mostly use soft-switching techniques. [5] proposes a novel soft-switching topology for zeta–fly-back converter. [6] proposes a

bidirectional dc–dc converter topology with dual half-bridge topology which has the advantage over dual full-bridge topology in terms of reduced device count. [7] proposes a bidirectional fly-back dc–dc converter with ZCS. The soft-switching topologies give higher efficiency at the cost of increased device count. Higher device count also reduces the reliability of the circuit. Now, if multiple batteries are to be connected in parallel to increase the total energy storage capacity, it is not possible by connecting the terminals of two batteries in parallel. This leads to the option of multiphase converter topology. Apart from giving the flexibility of paralleling multiple batteries, it also increases the fault-tolerant capacity, i.e., if one of the phases fails, then other phases can still operate, and the whole system will not come to a halt. [8] proposes a bidirectional dc–dc converter with many interleaved buck stages for automotive application. Apart from multiphase operation, the power converter should also be able to interface multiple energy sources to the battery. [9] proposes a scheme where multiple energy sources and the battery are connected to the dc bus, and the dc bus works as a junction point for all energy transfer.

II. CONCEPT OF FOUR PHASE BI-DIRECTIONAL FLYBACK CONVERTER

The basic block diagram of the prototype of the multi power port (MPP) which is built for hybrid electric vehicle application is shown in Figure 1. The heart of the circuit is the bidirectional fly-back dc–dc converter. A four-phase converter is constructed. The power schematic of the bidirectional dc–dc converter is shown in Figure 2. It has four identical bidirectional fly back dc–dc converters. Each converter has an individual battery, and all the converters are connected to the common dc bus. If we consider the first converter, then, during forward power flow S1 and D2 are active and during reverse power flow,

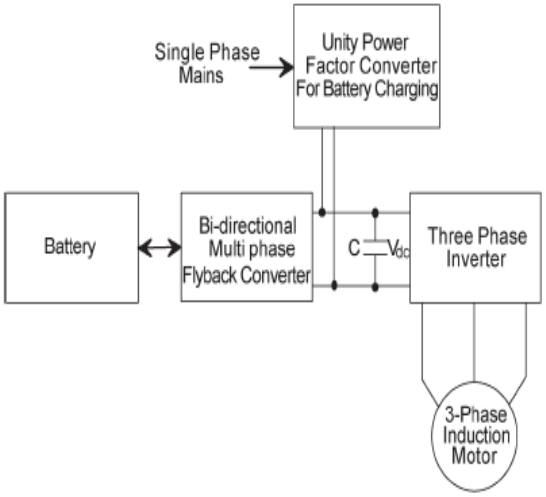

Figure 1. Block diagram of the proposed power schematic

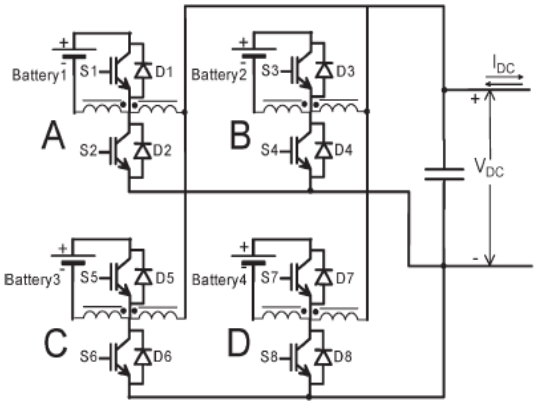

Figure 2: Four-phase bidirectional fly-back converter

S2 and D1 are active as well. During forward power flow, active switches S1, S3, S5, and S7 get switching pulses of 75% duty cycle with 90◦ phase difference between subsequent phases, as shown in Fig. 3(a). During reverse power flow, active switches S2, S4, S6, and S8 get switching pulses of 25% duty cycle which are 90◦ phase shifted to each other, as shown in Figure 3(b). Figure 3(c) and (d) shows the ideal switch voltage and current waveforms assuming continuous conduction mode (CCM) for forward and reverse power flows, respectively. CCM is not the only conduction mode for this bidirectional converter.

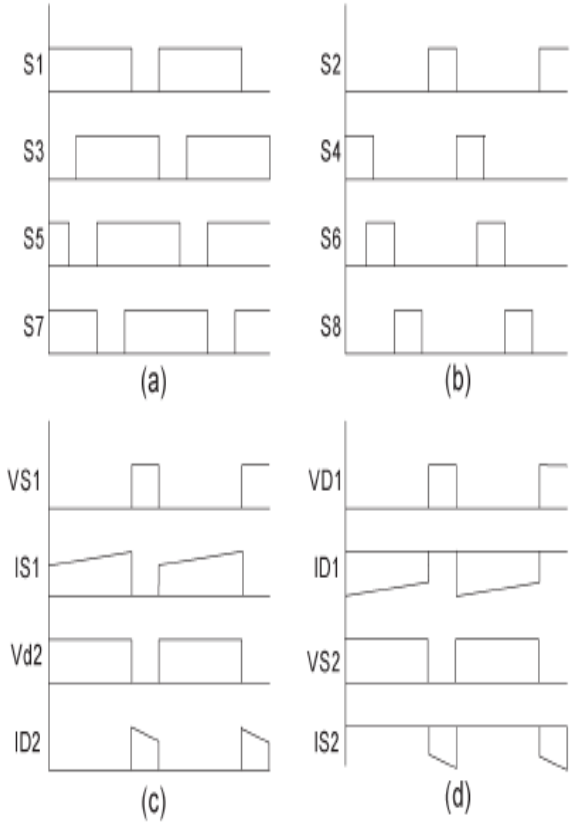

Figure 3: (a) Switching pulses during forward power flow. (b) Switching pulses during reverse power flow. (c) Ideal switch voltage and current waveforms during forward power flow for phase A assuming continuous conduction. (d) Ideal switch voltage and current waveforms during reverse power flow for phase A assuming continuous conduction.

This can also operate in critical conduction mode (CRM) or discontinuous conduction mode (DCM), depending on the load. During forward power flow, if the load is very less, then the converter can go into CRM or DCM, similar to any standard fly-back converter. However, for circuit design, only CCM is considered. As no snubber is used, circuit design involves the design of the inductor and the capacitor. The load connected at the output of the converter is a three phase inverter connected to the motor. Thus, the capacitor voltage ripple is dominated by the dc link current ripple of the inverter, and capacitor value is decided depending on that ripple. The fly-back inductor value is selected such that the inductor current ripple is 10% of the full-load current during CCM. DCM and CRM are not considered for circuit design because there is no stringent voltage regulation requirement for the MPP output. The regulation is handled by the downstream inverter.

III. CONTROL SCHEME

Simple hysteresis voltage control is used for dc-link voltage regulation for power management in the proposed MPP scheme. During power flow in the forward direction, i.e., from the battery to the dc bus, the duty cycles of switching voltages of S1, S3, S5, and S7 are fixed at 75%, while switches S2, S4, S6, and S8 are permanently off. During reverse power flow, S1, S3, S5, and S7 are permanently off, and S2, S4, S6, and S8 are switched at 25% duty cycle. Therefore, during forward power flow, the voltage is boosted by a factor of three, and during reverse power flow, the voltage is stepped down by a factor of three. It is to be noted that this voltage boost is only due to duty-cycle operation. The coupled-inductor turns ratio is fixed in such a way that during full-load operation in forward mode, the converter output voltage is the rated dc bus voltage V_{dc}. For an operating condition with lesser load, the series voltage drop in the converter will be less. Thus, the dc-link voltage will get increased from the rated value because of fixed duty cycle of operation. At a voltage $V_{dc} + v_1$, the pulses to switches S1, S3, S5, and S7 are stopped. If the load is still drawing current, then it will discharge the capacitor. When the voltage reaches V_{dc}, again, the switching pulses are given to S1, S3, S5, and S7. Therefore, during light-load conditions, the voltage is maintained between V_{dc} and $V_{dc} + v_1$. If there is no load, then the voltage will also be maintained in between V_{dc} and $V_{dc} + v_1$.

However, during regeneration, even if switches S1, S3, S5, and S7 are off, because of reverse power flow, the voltage will increase beyond $V_{dc} + v_1$. This is the time when energy should flow back to the battery. Thus, at a voltage $V_{dc} + v_1 + v_2$, switches S2, S4, S6, and S8 are pulsed, and because of the flyback action, current flows into the battery, and the battery gets charged. Here also, if the capacitor voltage falls below $V_{dc} + v_1$, the pulses to switches S2, S4, S6, and S8 are stopped. In this way, during regeneration, the voltage is maintained above $V_{dc} + v_1$. Here, the upper limit of the dc bus voltage is not fixed. It can be more than $V_{dc} + v_1 + v_2$ also if very high regenerative current flows. However, the rate at which the converter feeds current to the battery can be less because of fixed duty cycle of operation. Therefore, the capacitor voltage can shoot up to a very high value. The dynamic resistance of the inverter provides the necessary protection at this operating condition. The dynamic resistance of the inverter is activated when the capacitor voltage reaches $V_{dc} + v_1 + v_2 + v_3$. The dynamic resistor can be switched off when the capacitor voltage decreases below $V_{dc} + v_1 + v_2$. This same control scheme is exploited during the battery-charging operation. For battery charging, the front-end converter is designed to maintain a voltage more than $V_{dc} + v_1 + v_2$ but less than $V_{dc} + v_1 + v_2 + v_3$. Thus, automatically, the reverse-power-flow operation gets activated, and the battery gets charged.

IV. MATHEMATICAL MODEL OF INDUCTION MOTOR DRIVE

The induction machine d-q or dynamic equivalent circuit is shown in Fig. 3 and 4. One of the most popular induction motor models derived from this equivalent circuit is Krause's model detailed in [5]. According to his model, the modeling equations in flux linkage form are as follows:

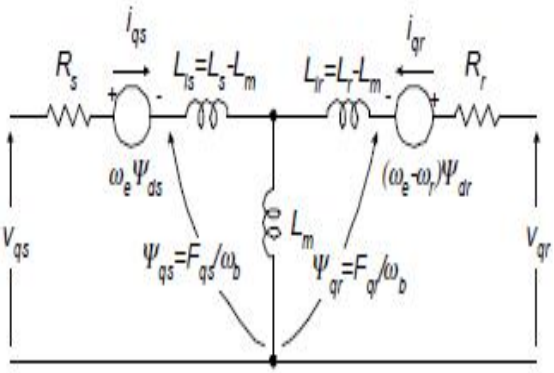

Figure 4: Dynamic q-axis model

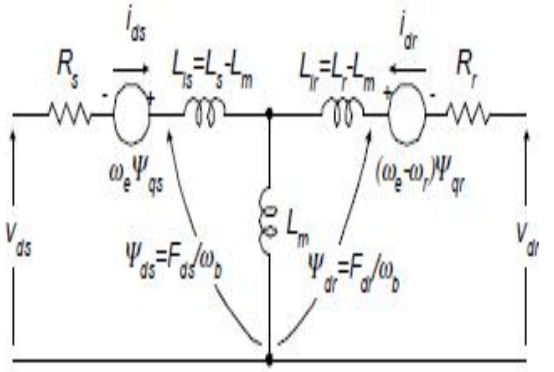

Figure 5: Dynamic d-axis model

$$\frac{dF_{qs}}{dt}=\omega_b\left[v_{qs}-\frac{\omega_e}{\omega_b}F_{ds}+\frac{R_s}{x_{ls}}\left(F_{mq}+F_{qs}\right)\right] \quad (1)$$

$$\frac{dF_{ds}}{dt}=\omega_b\left[v_{ds}+\frac{\omega_e}{\omega_b}F_{qs}+\frac{R_s}{x_{ls}}\left(F_{md}+F_{ds}\right)\right] \quad (2)$$

$$\frac{dF_{qr}}{dt}=\omega_b\left[v_{qr}-\frac{(\omega_e-\omega_r)}{\omega_b}F_{dr}+\frac{R_r}{x_{lr}}\left(F_{mq}-F_{qr}\right)\right] \quad (3)$$

$$\frac{dF_{dr}}{dt}=\omega_b\left[v_{dr}+\frac{(\omega_e-\omega_r)}{\omega_b}F_{qr}+\frac{R_r}{x_{lr}}\left(F_{md}-F_{dr}\right)\right] \quad (4)$$

$$F_{mq}=x_{ml}^{*}\left[\frac{F_{qs}}{x_{ls}}+\frac{F_{qr}}{x_{lr}}\right] \quad (5)$$

$$F_{md}=x_{ml}^{*}\left[\frac{F_{ds}}{x_{ls}}+\frac{F_{dr}}{x_{lr}}\right] \quad (6)$$

$$i_{qs}=\frac{1}{x_{ls}}\left(F_{qs}-F_{mq}\right) \quad (7)$$

where d : direct axis,
q : quadrature axis,
s : stator variable,
r : rotor variable,
F_{ij} is the flux linkage (i=q or d and j=s or r),
v_{qs}, v_{ds} : q and d–axis stator voltages,
v_{qr}, v_{dr} : q and d–axis rotor voltages,
F_{mq},F_{md} : q and d axis magnetizing flux linkages,
Rr : rotor resistance,
Rs : stator resistance,
X_{ls} : stator leakage reactance ($\omega_e L_{ls}$),
X_{lr} : rotor leakage reactance ($\omega_e L_{lr}$),

$$X_{ml}^{*}: 1\Big/\left(\frac{1}{x_m}+\frac{1}{x_{ls}}+\frac{1}{x_{lr}}\right),$$

i_{qs}, i_{ds} : q and d–axis stator currents,
i_{qr}, i_{dr} : q and d–axis rotor currents,
p : number of poles,
J : moment of inertia,
T_e : electrical output torque,
T_L(or T_l) : load torque,
ω_e : stator angular electrical frequency,
ω_b : motor angular electrical base frequency,
ω_r : rotor angular electrical speed.

$$i_{ds}=\frac{1}{x_{ls}}\left(F_{ds}-F_{md}\right) \quad (8)$$

$$i_{qr}=\frac{1}{x_{lr}}\left(F_{qr}-F_{mq}\right) \quad (9)$$

$$i_{dr}=\frac{1}{x_{lr}}\left(F_{dr}-F_{md}\right) \quad (10)$$

$$T_e=\frac{3}{2}\left(\frac{p}{2}\right)\frac{1}{\omega_b}\left(F_{ds}i_{qs}-F_{qs}i_{ds}\right) \quad (11)$$

$$T_e-T_L=J\left(\frac{2}{p}\right)\frac{d\omega_r}{dt} \quad (12)$$

For a squirrel cage induction machine, as in the case of this paper, v_{qr} and v_{dr} in (3) and (4) are set to zero. An induction machine model can be represented with five differential equations as shown. To solve these equations, they have to be rearranged in the state-space form, In this case, state-space form can be achieved by inserting (5) and (6) in (1–4) and collecting the similar terms together so that each state derivative is a function of only other state variables and model inputs. Then, the modeling equations (1-4) of a squirrel cage induction motor in state-space become

$$\frac{dF_{qs}}{dt}=\omega_b\left[v_{qs}-\frac{\omega_e}{\omega_b}F_{ds}+\frac{R_s}{x_{ls}}\left(\frac{x_{ml}^{*}}{x_{lr}}F_{qr}+\left(\frac{x_{ml}^{*}}{x_{ls}}-1\right)F_{qs}\right)\right] \quad (13)$$

$$\frac{dF_{ds}}{dt}=\omega_b\left[v_{ds}+\frac{\omega_e}{\omega_b}F_{qs}+\frac{R_s}{x_{ls}}\left(\frac{x_{ml}^{*}}{x_{lr}}F_{dr}+\left(\frac{x_{ml}^{*}}{x_{ls}}-1\right)F_{ds}\right)\right] \quad (14)$$

$$\frac{dF_{qr}}{dt}=\omega_b\left[-\frac{(\omega_e-\omega_r)}{\omega_b}F_{dr}+\frac{R_r}{x_{lr}}\left(\frac{x_{ml}^{*}}{x_{ls}}F_{qs}+\left(\frac{x_{ml}^{*}}{x_{lr}}-1\right)F_{qr}\right)\right] \quad (15)$$

$$\frac{dF_{dr}}{dt}=\omega_b\left[\frac{(\omega_e-\omega_r)}{\omega_b}F_{qr}+\frac{R_r}{x_{lr}}\left(\frac{x_{ml}^{*}}{x_{ls}}F_{ds}+\left(\frac{x_{ml}^{*}}{x_{lr}}-1\right)F_{dr}\right)\right] \quad (16)$$

$$\frac{d\omega_r}{dt}=\left(\frac{p}{2J}\right)\left(T_e-T_L\right) \quad (17)$$

V. MATLAB/SIMULINK MODELLING AND SIMULATION RESULTS

Here the simulation is carried out by two cases 1. Proposed Four-phase bidirectional fly-back converter

2. Proposed Four-phase bidirectional fly-back converter Applied to induction motor drive.

Case 1: Proposed Four-phase bidirectional fly-back converter:

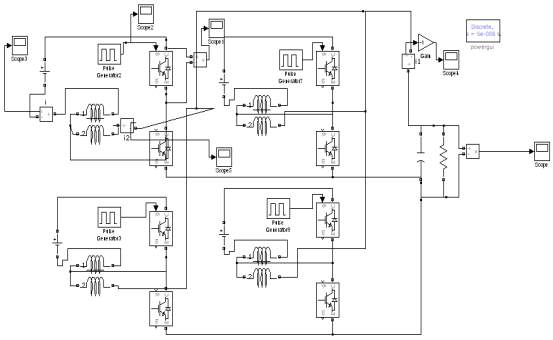

Figure 6: Matlab/Simulink model of Proposed Four-phase bidirectional fly-back converter without soft sort

Figure 6 shows the Matlab/Simulink model of Proposed Four-phase bidirectional fly-back converter without soft sort.

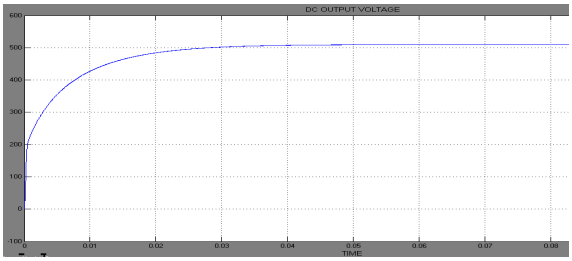

Figure 7: Output Voltage of the fly-back converter

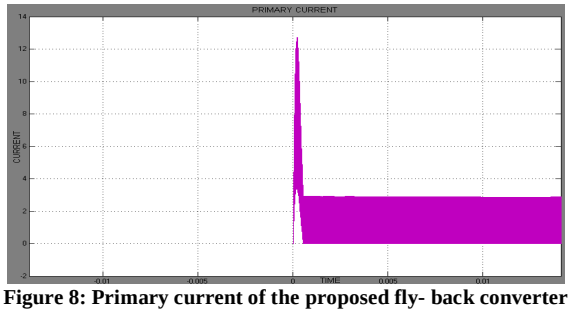

Figure 8: Primary current of the proposed fly- back converter without soft sort

Figure 7 and 8 shows the DC link voltage and Primary current of the proposed fly back converter without soft sort.

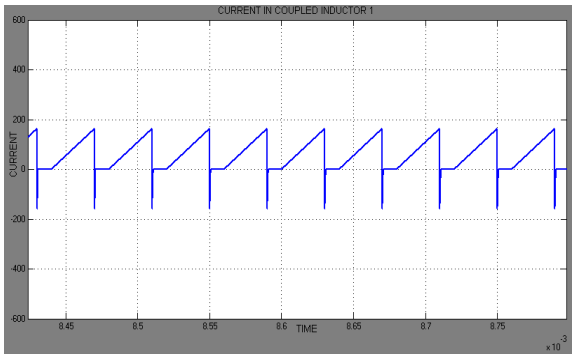

Figure 9: Current flowing in the coupled inductor

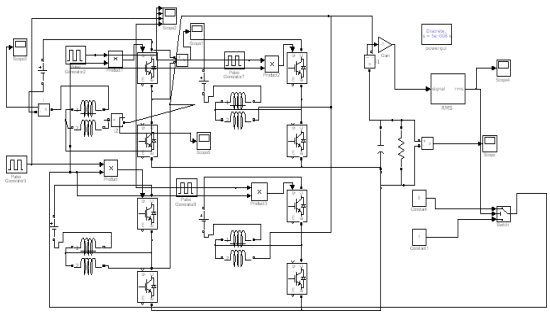

Figure 10: Matlab/Simulink model of Proposed Four-phase bidirectional fly-back converter with soft sort

Figure 10 shows the Matlab/Simulink model of Proposed Four-phase bidirectional fly-back converter with soft sort

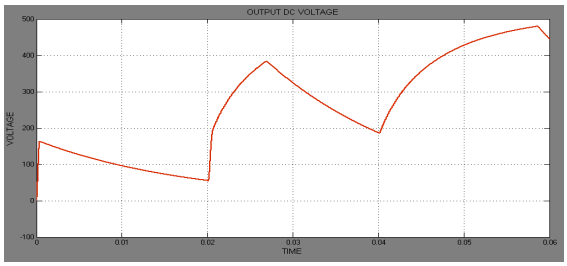

Figure 11: Output Voltage of the fly-back converter in soft sort

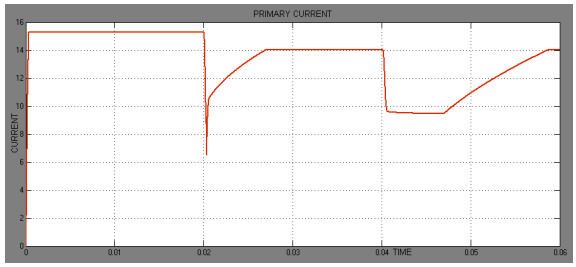

Figure 12: Primary Current of the fly back converter in soft sort

Figure 11 and 12 shows the DC Output voltage and primary current of the proposed fly back converter in soft sort method.

Case 2:. Proposed Four-phase bidirectional fly-back converter Applied to induction motor drive

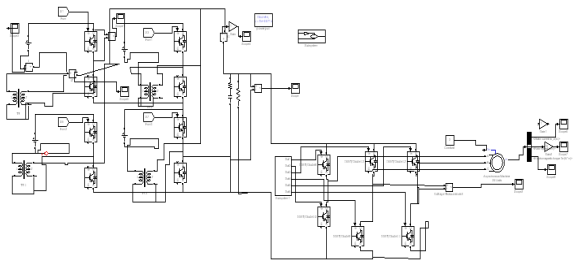

Figure 13: Matlab/Simulink Model of Proposed Four-phase bidirectional fly-back converter Applied to induction motor drive

Figure 13 shows the Matlab/Simulink model of Proposed Four-phase bidirectional fly-back converter

Applied to induction motor drive interfacing by using the DC to AC converter. To check the performance of the induction motor drive.

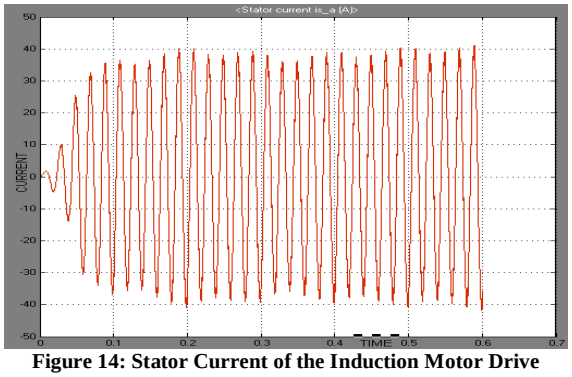

Figure 14: Stator Current of the Induction Motor Drive

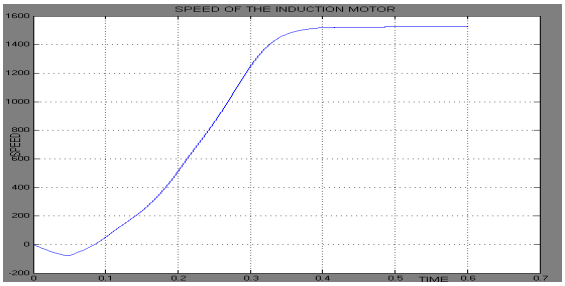

Figure 15: Speed of the Induction Motor

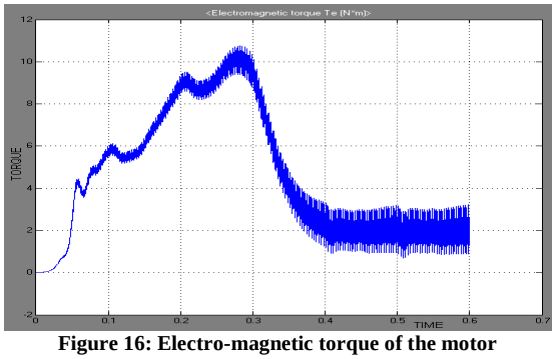

Figure 16: Electro-magnetic torque of the motor

Figure 14, 15, 16 Shows the Induction drive Performance Characteristics, Armature current, Speed , Electromagnetic Torque of the drive respectively.

V. CONCLUSION

This paper proposes a four-phase bidirectional fly-back dc–dc converter which serves the role of an MPP interface for electric and hybrid electric vehicle applications. The bidirectional nature of the converter allows battery charging during regeneration and also from mains. The multiple phases give the flexibility of paralleling multiple batteries. Simple hysteresis control is used for converter control. Because of the four converters operating with 90◦ phase shift with fixed 75% duty cycle of operation, the capacitor ripple current is also reduced. The novel transformer design technique drastically reduces the leakage inductance and eliminates the requirement of snubber. And same system is applied to Induction Motor Drive with the help of the interfacing inverter and to check the performance characteristics of system ,and drive.

REFERENCES

[1] A. Emadi, Y. J. Lee, and K. Rajashekara, "Power electronics and motordrives in electric, hybrid electric, and plug-in hybrid electric vehicles," *IEEE Trans. Ind. Electron.*, vol. 55, no. 6, pp. 2237–2245, Jun. 2008.

[2] F. Caricchi, F. Crescimbini, G. Noia, and D. Pirolo, "Experimental study of a bidirectional DC–DC converter for the DC link voltage control and the regenerative braking in PM motor drives devoted to electrical vehicles," in *Proc. IEEE APEC*, Orlando, FL, Feb. 1994, vol. 1, pp. 381–386.

[3] F. Caricchi, F. Crescimbini, F. G. Capponi, and L. Solero, "Study of bi-directional buck–boost converter topologies for application in electrical vehicle motor drives," in *Proc. IEEE APEC*, Feb. 1998, vol. 1, pp. 287–293.

[4] C.-M. Wang, "Novel zero-voltage-transition PWM DC–DC converters," *IEEE Trans. Ind. Electron.*, vol. 53, no. 1, pp. 254–262, Feb. 2006.

[5] B.-R. Lin and F.-Y. Hsieh, "Soft-switching zeta–flyback converter with a buck–boost type of active clamp," *IEEE Trans. Ind. Electron.*, vol. 54, no. 5, pp. 2813–2822, Oct. 2007.

[6] F. Z. Peng, H. Li, G.-J. Su, and J. S. Lawler, "A new ZVS bidirectional DC–DC converter for fuel cell and battery application," *IEEE Trans. Power Electron*, vol. 19, no. 1, pp. 54–65, Jan. 2004.

[7] H. S.-H. Chung, W.-L. Cheung, and K. S. Tang, "A ZCS bidirectional flyback DC/DC converter," *IEEE Trans. Power Electron*, vol. 19, no. 6, pp. 1426–2434, Nov. 2004.

[8] O. Garcia, P. Zumel, A. de Castro, and J. A. Cobos, "Automotive DC–DC bidirectional converter made with many interleaved buck stages," *IEEE Trans. Power Electron.*, vol. 21, no. 6, pp. 578–586, May 2006.

[9] L. Solero, A. Lidozzi, and J. A. Pomilio, "Design of multiple-input power converter for hybrid vehicles," in *Proc. IEEE APEC*, vol. 2, pp. 1145–1151.

[10] M. Michon, J. L. Duarte, and M. Hendrix, "A three port bi-directional converter for hybrid fuel cell systems," in *Proc. IEEE PESC*, Aachen, Germany, Jun. 2004, pp. 4736–4742.

[11] H. Tao, A. Kotsopoulos, J. L. Duarte, and M. A. M. Hendrix, "Family of multiport bidirectional DC–DC converters," *Proc. Inst. Elect. Eng.—Electr. Power Appl.*, vol. 153, no. 3, pp. 451–458, May 2006.

[12] R.-J. Wai, L.-W. Liu, and R.-Y. Duan, "High-efficiency voltage-clamped DC–DC converter with reduced reverse-recovery current and switch voltage stress," *IEEE Trans. Ind. Electron.*, vol. 53, no. 1, pp. 272–280, Feb. 2006.

[13] R.-J. Wai, C.-Y. Lin, R.-Y. Duan, and Y.-R. Chang, "High-efficiency DC–DC converter with high voltage gain and reduced switch stress," *IEEE Trans. Ind. Electron.*, vol. 54, no. 1, pp. 354–364, Feb. 2007.

[14] T. Bhattacharya, V. S. Giri, K. Mathew, and L. Umanand, "Multi power port converter for hybrid electric vehicles using multi phase bidirectional fly-back topology," in *Proc. IEEE ICIT*, Dec. 2006, pp. 1201–1205.

◈◈◈